Nicolas Oppmann*
Andreas Jess

# Improving the Selectivity to Liquefied Petroleum Gas by Combining Fischer-Tropsch Synthesis with Zeolite Cracking

The Fischer-Tropsch synthesis (FTS) is a heterogeneously catalyzed surface polymerization reaction with a wide spectrum of hydrocarbons as products, following the Anderson-Schulz-Flory distribution. Subsequent cracking of the unwanted long-chain products can increase the desired product fraction of shorter hydrocarbons (HCs). In this work, a Co/Mn-catalyzed FTS with additional cracking by a Pt/H-ZSM-5 zeolite was investigated to increase the selectivity of liquefied petroleum gas (LPG). At lower zeolite temperatures, no cracking but isomerization and the conversion of alcohols took place. Raising the temperature of the cracking process resulted in cracking of long-chain HCs and increased the total LPG selectivity. Additional experiments by cracking of *n*-hexadecane as model substance were conducted.



Supporting Information available online

**Keywords:** Fischer-Tropsch synthesis, *n*-Hexadecane, H-ZSM-5, Liquefied petroleum gas, Zeolite cracking

*Received:* September 16, 2022; *revised:* December 14, 2022; *accepted:* January 13, 2023

**DOI:** 10.1002/ceat.202200445

## 1 Introduction

Climate change due to the anthropogenic emission of greenhouse gases by the combustion of fossil fuels is one of the main global problems mankind is facing [1]. This makes it necessary to abandon fossil fuels as soon as possible and search for clean and renewable energy sources. To solve this problem, the production of fuels by means of Fischer-Tropsch synthesis (FTS) becomes an alternative [2–5]. The reaction allows producing mainly linear hydrocarbons (HCs) by the conversion of syngas ($CO + H_2$) [6]. The FT reaction can be regarded as a surface catalyzed polymerization, i.e., by a chain propagation mechanism in which methylene units are consecutively incorporated:

$$n\mathrm{CO} + 2n\mathrm{H_2} \rightarrow (-\mathrm{CH_2}-)_n + n\mathrm{H_2O} \quad (1)$$

By the use of renewable produced hydrogen by water electrolysis and $CO_2$ (e.g., separated from flue gases of power plants, steel/cement production, chemical industry, from biogas, or in future even from air) as carbon source, this process will emit much less $CO_2$ than traditional fuels based on crude oil [7].

One of the largest proton exchange membrane (PEM) electrolyzers in Europe was just recently built in Wunsiedel (start-up in September 2022), a small city in Upper Franconia (northern Bavaria), with a capacity of 1350 t of green hydrogen per year [8]. Besides the direct use of $H_2$ by a local gas company, excess hydrogen can be utilized for the production of hydrocarbons (HCs) by FTS. Hence, about 3200 t of HCs per year could be theoretically produced by FTS, if the $H_2$ is partly, i.e., about 1/3, converted by the reverse water-gas shift reaction ($CO_2 + H_2 \rightleftharpoons CO + H_2O$) to produce the CO needed for the FTS. Due to a high demand of liquefied petroleum gas (LPG) in this rural area as fuel in households and small businesses, the selectivity enhancement of LPG in this reaction is of great interest.

Besides all advantages of FTS, there is one major drawback. The kinetics of the FTS, which can be regarded as a heterogeneously catalyzed surface polymerization reaction, results in a statistical distribution of HCs, known as Anderson-Schulz-Flory distribution (ASF), characterized by the chain growth probability $\alpha$[1)] [9, 10]. The selectivity towards LPG ($C_3 + C_4$ fraction) is therefore limited to a theoretical maximum of $\approx 32\,\mathrm{wt_C\,\%}$ (Fig. 1) at $\alpha \approx 0.55$ considering the following assumptions: (i) only chain growth reactions take place and no cracking occurs; (ii) both methane and $C_2$ also follow the ASF distribution. To overcome this limitation of FTS and to increase the LPG selectivity, cracking of the longer chain compounds on acid zeolites is an option [11–15].

There are numerous investigations focusing on a hybrid concept of FT and zeolite catalyst in a single step for improving

1) List of symbols at the end of the paper.

Nicolas Oppmann, Prof. Dr.-Ing. Andreas Jess
(Nicolas1.oppmann@uni-bayreuth.de)
University of Bayreuth, Department of Chemical Engineering, Center of Energy Technology (ZET), Universitaetsstrasse 30, 95447 Bayreuth, Germany.

  

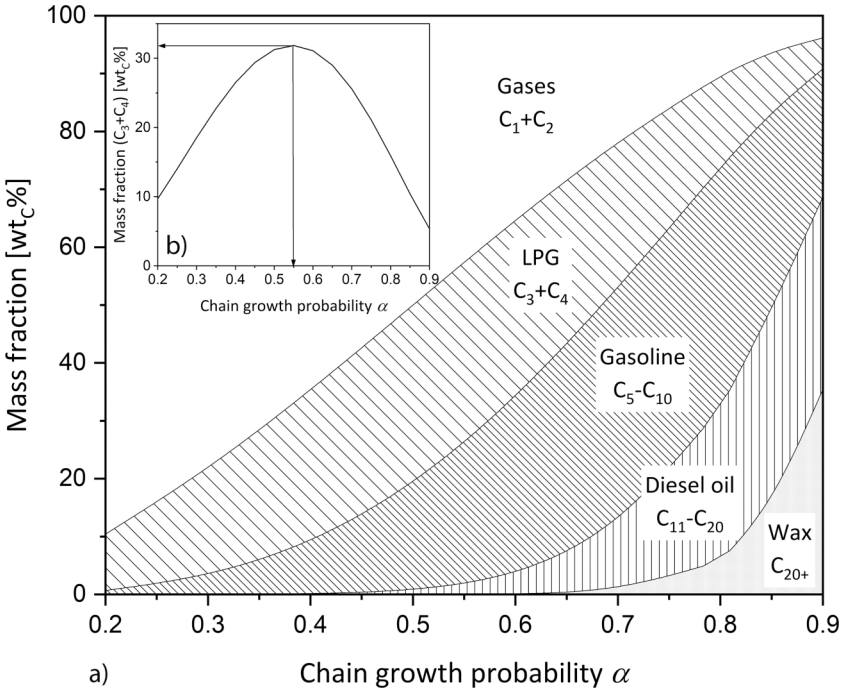


**Figure 1.** (a) Mass fraction on carbon basis of typical product fractions of Fischer-Tropsch synthesis with a varying chain growth probability $\alpha$. (b) Mass fraction of LPG ($C_3$ + $C_4$) with varying $\alpha$. Note that $\alpha$ values < 0.5 are not likely for FTS and are only shown for the sake of completeness/comparison.

selectivity of gasoline range hydrocarbons. Namely, these concepts are physically mixing both catalysts, zeolite-supported FT catalysts and zeolite encapsulated FT catalysts [16]. Also dual-bed configurations are investigated in which both catalysts are separated in one reactor [17–19]. However, single-stage arrangements suffer from the disadvantage that at least one catalyst must operate under less than optimal conditions. Therefore, two-stage operation is performed for downstream processing of FT products [20].

Multiple combinations of FT and acidic catalysts for downstream FT product conversion have been tested, many focusing on the increase of the gasoline fraction of hydrocarbons [21–25]. Little research is done to improve the selectivity of LPG from an FTS/zeolite process [11, 26], as LPG is often regarded as low-value product. Nevertheless, the sustainable production of LPG from non-petroleum sources is of great importance and the key objective of this paper. This work is of great interest, as we want to determine the optimal process parameters for the production of LPG by the FTS/zeolite process.

Bifunctional hydrocracking on a catalyst having a (de)hydrogenation component, often a noble metal, and a Brønsted acid center is of advantage compared to catalytic cracking on monofunctional acid catalysts [27]. Marked differences are the lower reaction temperatures necessary for hydrocracking and the lower tendency for deactivation by coke precursors such as olefins and subsequent formation of carbonaceous deposits, respectively [28, 29].To achieve the highest overall selectivity for LPG by FTS combined with cracking, it is, from a theoretical point of few, better to run FTS not at the highest LPG selectivity ($\alpha$ = 0.55) but at higher $\alpha$ values, and thus with an initially higher yield of $C_{5+}$-HCs (and lower yield of LPG, respectively) in the first process step of FTS. These $C_{5+}$-HCs can then be subsequently cracked to LPG and therefore increase the overall LPG selectivity.

Lower $\alpha$ values (< 0.55) result in a high selectivity to methane and $C_2$ gases (ethene, ethane) which of course cannot be further converted to LPG by cracking. Until now, it is an open question, which $\alpha$ value of FTS and which configuration and reaction conditions such as temperature of FTS and cracking are optimal to achieve the highest LPG yield in a process combining FTS and cracking.

The present works aims to increase the selectivity of LPG of the combined process by using a Co/Mn-FT catalyst and a platinum-doped acid zeolite (Pt/H-ZSM-5) as cracking catalyst in different reactor setups. The FTS was thereby investigated with and without combination with cracking. The cracking reactions only were also studied by using *n*-hexadecane ($C_{16}H_{34}$) as model substance for $C_{5+}$-HCs typically formed by FTS.

## 2 Experimental

### 2.1 Catalysts

#### 2.1.1 FTS Catalyst Preparation

Previous studies have shown that the promotor manganese increases the olefin (and alcohol) selectivity of Co-based FT catalysts significantly and also decreases the chain growth probability [30]. Hence, for the FTS experiments, a cobalt-manganese catalyst (20 wt% Co, 3 wt% Mn, amount of reduced metal on final catalyst) with a high yield of $\alpha$ olefins was used [30], as olefins show a higher reactivity for cracking reactions as the initial step of dehydrogenation is not required [31].

The catalyst was prepared by wet impregnation. The dry $SiO_2$ support material (Aerolyst 3041, extruded cylinders, $d_P$ = 1.6 mm, 12 h, 110 °C) was impregnated with an aqueous solution containing a mixture of the required amounts of $Co(NO_3)_2{\cdot}6H_2O$ and $Mn(NO_3)_2{\cdot}4H_2O$. Therefore, a solution of the calculated amounts of metal salts in water ($6\ mL_{H2O}g_{support\ material}^{-1}$) was prepared and the support material was added. After removing the solvent at 60 °C under reduced pressure in a rotary evaporator (1 h 300 mbar, 1 h 200 mbar, 1 h 100 mbar, 12 h 40 mbar), the solid was calcined by heating up in flowing air in a fixed-bed reactor ($3\ K\ min^{-1}$, 360 °C, 3 h hold, airflow of $1.5\ L\ h^{-1}g_{cat.}^{-1}$). To avoid internal transport limitations (pore effectiveness factor < 1) during the reaction, the FT catalyst was crushed and sieved to particles with $d_P$ < 90 µm.

  

### 2.1.2 Zeolite Preparation

The ammonium form of ZSM-5 zeolite ($NH_4^+$-ZSM-5, $SiO_2/Al_2O_3$ = 30) was purchased as powder from Thermo Scientific. To achieve the active protonic form (H-ZSM-5), the sample was calcined in a fixed-bed reactor at 500 °C in $N_2$ flow for 5 h (3 K min$^{-1}$, 2.0 L h$^{-1}$ $g_{zeolite}^{-1}$). The high temperature forms $NH_3$, leaving behind the protonic form $H^+$-ZSM-5, denoted as H-ZSM-5. An ion exchange method was used to impregnate the activated H-ZSM-5 with 0.5 wt % Pt (amount of reduced metal on final zeolite). Therefore, the appropriate amount of $[Pt(NH_3)_4](NO_3)_2$ was dissolved in water (3.5 $mL_{H2O}$ $g_{zeolite}^{-1}$) and the zeolite added. The ion exchange was carried out for 24 h at 25 °C. After evaporating the solvent under reduced pressure in a rotary evaporator under the same conditions as for the FT catalyst, the calcination was carried out in a fixed-bed reactor, by slowly heating up the sample (0.2 K min$^{-1}$, 350 °C, flowing air 2.0 L h$^{-1}$ $g_{zeolite}^{-1}$).

## 2.2 Reactor System

All experiments were carried out in fixed-bed reactors with an inner diameter of 14 mm. For isothermal conditions in axial direction the stainless-steel reactors were enclosed in an aluminum block and the temperature was controlled by electrical heating jackets. The isothermal conditions of the reactor in axial direction were analyzed and the results are displayed in Fig. S3 in the Supporting Information. A detailed scheme of the experimental setups is illustrated in Fig. 2.

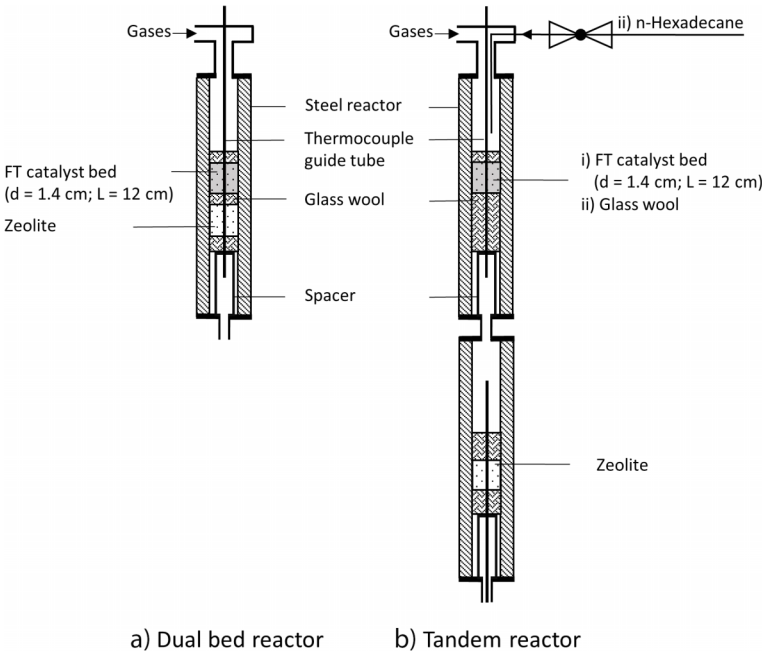


**Figure 2.** (a) Dual-bed reactor setup with catalyst beds physically separated by a layer of glass wool. (b) Tandem reactor setup with two independent heatable reactors. The tandem reactor setup can be used for (i) FTS/zeolite reactions and (ii) *n*-hexadecane/zeolite experiments. In both cases the spacer is used to ensure a defined position of the catalyst bed in the reactor.

Gas flows were controlled by Bronkhorst mass flow controllers. During the experiments the outflowing gas passed through a trap heated to 180 °C and maintained at reaction pressure, to condense the heavy waxes of the reaction. After pressure relief to ambient pressure, the gas stream was bubbled through an iced washing bottle filled with toluene to wash out the longer HCs. The products were collected for 4–6 h and the samples of both separators were combined and quantified by adding cyclooctane as internal standard and measured by gas chromatography (GC). After the washing bottle, an internal standard of 1 vol % cyclopropane in $N_2$ was introduced into the product gas. By the use of cyclopropane, it was possible to quantify the HCs still present, also by GC. The gases then passed a cold trap (–80 °C) and the gas composition (CO, $CO_2$, $CH_4$, $H_2$) was detected with a gas analyzer. A soap bubble burette to measure the volume flows was installed at the end.

Prior to the reactions, the catalysts were activated by heating in 20 vol % $H_2$ in $N_2$ (3 K min$^{-1}$ to 360 °C with 3 h hold) and then kept for 2 h at 360 °C in pure hydrogen. After reduction, the temperature was lowered to 150 °C and syngas ($CO/H_2$ volume ratio of 1:2) was used to raise the reactor pressure to 20 bar. Then the reactor temperature was increased to the selected value. The reactor system was either operated as one reactor with two catalyst beds (at the same temperature), or as two subsequent reactors (tandem setup) with the option of running FTS and cracking at different temperatures. To study FTS or cracking only, the reactor was loaded either only with the FT or the cracking catalyst, respectively.

### 2.2.1 Fischer-Tropsch Experiments

In a typical experiment, the upper reactor was loaded with a mixture of FT catalyst and quartz sand (constant bed volume of 18 cm$^3$) to avoid local temperature hot spots. For dual-bed experiments, the zeolite was firstly loaded in the reactor and physically separated from the FT catalyst by a layer of glass wool. This setup is presented in Fig. 2a. For tandem reactor experiments, the reactor containing the zeolite is connected directly to the FT reactor in down flow direction as shown in Fig. 2b mode (i). In all experiments, the reactor pressure and gas composition are constant and only the temperature was changed.

To assure steady-state conditions of the FT reaction, the FTS was run for 48 h after reduction and also after every change of reaction conditions. In Fig. S4, both the reaction rate of CO and $\alpha$ as a function of time-on-stream are depicted, which supports the assumption of steady-state conditions after 48 h.

### 2.2.2 Model Substance Experiments

For cracking experiments with *n*-hexadecane as model substance, the reactor setup displayed in Fig. 2b mode (ii) was used. *n*-Hexadecane is liquid

  

at ambient temperatures and atmospheric pressure and has to be vaporized prior to reaction. For this, the upper reactor is only filled with glass wool and used as vaporizer at a temperature of 350 °C. An HPLC pump was employed to feed the desired amount of *n*-hexadecane into the vaporizer.

### 2.3 Calculations

The carbon mass-based fraction of the chain product *i* is represented by Eq. (2) defined as ASF distribution:

$$\omega_{C,i} = i\,\alpha^{i-1}(1-\alpha)^2 \tag{2}$$

where *i* defines the carbon number of the HC and $\alpha$ the chain growth probability factor.

The logarithmic representation of Eq. (2) leads to Eq. (3), and the chain growth probability can be determined by the slope of the linear regression line of the measured mass fraction. For the calculation only the $C_{3+}$-HCs are used, as methane and $C_2$ often do not follow the ASF distribution [32]. It must be made clear once again that the calculation of $\alpha$ can only be applied for mere FTS without zeolite cracking.

$$\log\left(\frac{\omega_{C,i}}{i}\right) = i\log(\alpha) + \log\left(\frac{(1-\alpha)^2}{\alpha}\right) \tag{3}$$

The carbon-related selectivity $S_i$ was calculated by Eq. (4):

$$S_i = \frac{\dot{m}_{C,i}}{\dot{m}_{C,total}} \tag{4}$$

with *i* is the carbon number of HC or carbon fraction (e.g., $C_{3+4} = C_3 + C_4$).

The conversion $X_i$ was calculated using Eq. (5):

$$X_i = \frac{\dot{n}_{i;in} - \dot{n}_{i;out}}{\dot{n}_{i;in}} = \frac{\dot{m}_{C,i;in} - \dot{m}_{C,i;out}}{\dot{m}_{C,i;in}} \tag{5}$$

with *i* = CO, *n*-hexadecane.

The modified residence time $\tau^*_{zeolite}$ is determined by Eq. (6):

$$\tau^*_{zeolite} = \frac{m_{zeolite}}{\dot{V}_{total}(p, T)} \tag{6}$$

The carbon mass flow $\dot{m}_{C,i}$ of each component *i* was calculated by Eq. (7):

$$\dot{m}_{C,i} = \dot{m}_{C,i;gas} + \frac{m_{C,i;liq.}}{t_{collection}} \tag{7}$$

where $t_{collection}$ is the time of product collection. The mass flow $\dot{m}_{C,i;gas}$ of components in the gas phase was quantified by a defined mass flow of cyclopropane introduced in the product gas flow. The mass flow of the liquid products $\dot{m}_{C,i;liq.}$ can be calculated by the mass of added cyclooctane and the time of product collection.

## 3 Results and Discussion

### 3.1 Variation of FTS Reaction Temperature

The selectivities and the corresponding chain growth probability factors $\alpha$ for an increasing FTS temperature are illustrated in Fig. 3. Note that the results of FTS only without subsequent cracking are shown and $\alpha$ is therefore calculated for FTS only. Increasing the FTS temperature leads to a decrease of the LPG selectivity from 36.3 $wt_C$ % (210 °C) to 18.5 $wt_C$ % (270 °C) and an increase of the $C_{5+}$ selectivity. As a result, the calculated $\alpha$ rises from 0.66 (210 °C) to 0.74 (270 °C) which do not agree with the model obtained by Vervloet et al. [33] for the dependency of $\alpha$ with temperature. Their model describes the selectivity by the ratio of chain propagation and termination reactions which show a standard Arrhenius dependency with temperature, meaning a decrease in $\alpha$ with rising temperature. However, this model is very simple and does not take into account that other side reactions take place, such as the re-adsorption and chain propagation of olefins built in the FT reaction.

Primarily formed $\alpha$-olefins can re-adsorb at the catalyst surface and initiate chain growth, forming HC chains that are indistinguishable from those formed from the direct reaction of CO and $H_2$ and eventually desorb as longer hydrocarbon chains. Furthermore, it is postulated that an increased re-adsorption of olefins will decrease the total chain termination probability [34, 35]. The used Co/Mn catalyst shows a high selectivity for olefins (44 $wt_C$ % at 210 °C) and the rise of temperature obviously leads to enhanced re-adsorption and thus chain propagation to longer HCs.

Taking only the FTS reaction into account, a lower temperature and therefore a lower $\alpha$ value would be beneficial for a high LPG selectivity. However, if also a subsequent cracking reaction is taken into consideration, it would be advantageous

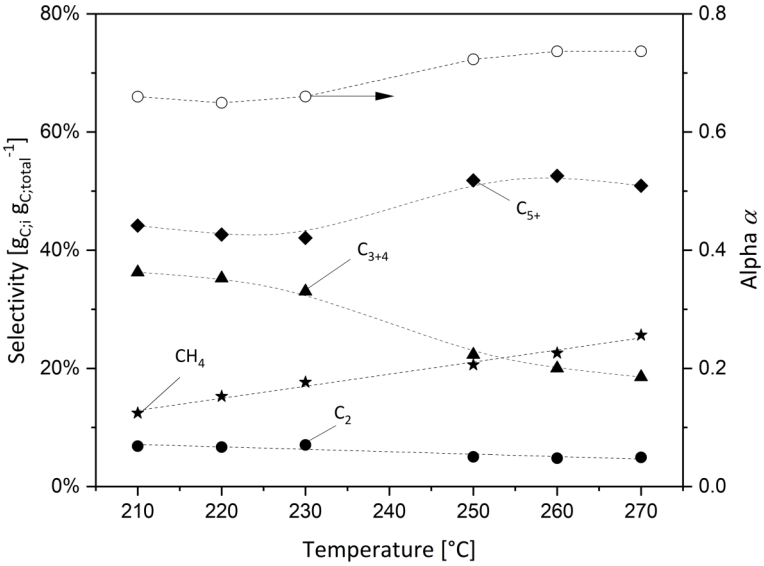


**Figure 3.** Influence of temperature on HC selectivities of FTS only. Corresponding $\alpha$ for each temperature is also shown ($p_{total}$ = 20 bar, $p_{H2}/p_{CO}$ = 2, $m_{catalyst}$ = 2.5 g (210–230 °C) or 0.19 g (240–270 °C), $X_{CO}$ = const. ≈ 13 %).

  

to drive the FTS to a higher $\alpha$ value to increase the yield of long-chain products available for cracking reactions. Therefore, a temperature of 260 °C (higher $\alpha$ value) was used for further FTS/zeolite experiments, i.e., for FTS combined with cracking.

Fig. 3 also depicts the selectivity of methane and $C_2$-HCs. Raising the temperature leads to a linear increase of the methane selectivity and decrease of $C_2$ selectivity. The formation of methane may be regarded as an independent reaction caused by an increased termination probability of the chain reaction [36] or a reaction on special active sites [37]. The high reactivity of ethene ($C_2$) is widely acknowledged as the reason for the negative deviation of the $C_2$ fraction from ASF distribution [35]. It is re-adsorbed and incorporated in the formation of longer hydrocarbons. An increase in temperature therefore leads to an increasing methane selectivity and decreasing $C_2$ selectivity due to enhanced re-adsorption. Both facts can lead to the already mentioned deviation of $C_1$ and $C_2$ from ASF distribution what can also be seen in Tab. 1. This deviation leads to higher selectivities for the $C_{3+4}$-fraction (e.g., FTS (210 °C) 36.3 $wt_C$ %, ASF distribution 28.4 $wt_C$ %) than theoretically possible by ASF distribution.

**Table 1.** HC selectivities of FTS compared with theoretical selectivities for the corresponding chain growth probability $\alpha$ according to ASF distribution. The $\alpha$ value was calculated using Eq. (3) and HC ≥ $C_3$. Linear regression for the calculation of $\alpha$ can be seen in Fig. S1 and Fig. S2.

| | $\alpha$ | Selectivity [$wt_C$ %] | | | |
|---|---|---|---|---|---|
| | | $CH_4$ | $C_2$ | $C_{3+4}$ | $C_{5+}$ |
| FTS (210 °C) | 0.66 | 12.4 | 6.8 | 36.3 | 44.2 |
| ASF distribution ($\alpha$ = 0.66) | 0.66 | 11.6 | 15.3 | 28.4 | 44.8 |
| FTS (260 °C) | 0.74 | 22.6 | 4.8 | 20.0 | 52.6 |
| ASF distribution ($\alpha$ = 0.74) | 0.74 | 6.8 | 10.0 | 22.1 | 61.2 |

## 3.2 Product Composition at Varying Temperatures for Dual Bed Setup

To increase the selectivity for LPG, a Pt/H-ZSM-5 zeolite was inserted downstream of the FT catalyst, physically separated by a layer of glass wool. The setup is denoted here as dual-bed setup. Within the experimental scatter of data, at a temperature of 210 °C, there were no differences in chain length distribution visible for the dual-bed run (Fig. 4b) compared to FTS only (Fig. 4a). However, no alcohols were present after the FTS products passed the zeolite in the dual-bed configuration. Hence, even at a rather low temperature of 210 °C the alcohols are dehydrated to paraffins and olefins with equal carbon number.

There was also a significant number of branched HCs detectable after the zeolite bed (dual-bed mode), especially olefins. This can be explained by reactions taking place at the zeolite surface. The 1-*n*-olefins adsorb at the acid sites of the zeolite and are present as carbenium ions, which undergo hydride shift or type 2 isomerization [38]. These isomerized olefins can desorb, isomerize again or be cleaved via type C cleavage. Since isomerization and desorption are much faster than type C cleavage, the latter plays a rather minor role at 210 °C.

In Fig. 5, the HC distributions for (a) FTS and (b) FTS/zeolite reaction is shown for a higher temperature of 260 °C both for FTS and cracking (compulsory for dual-bed mode). At this temperature, beside the isomerized olefins, also a significant amount of branched paraffins occur in the product spectrum. These branched alkanes must have been formed by hydrogenation of previously formed branched alkenes on the Pt sites, due to the reaction pathway of bifunctional hydrocracking. Pt is widely known to be a strong (de)hydrogenation catalyst, but its activity seems here to be weakened, since a significantly higher

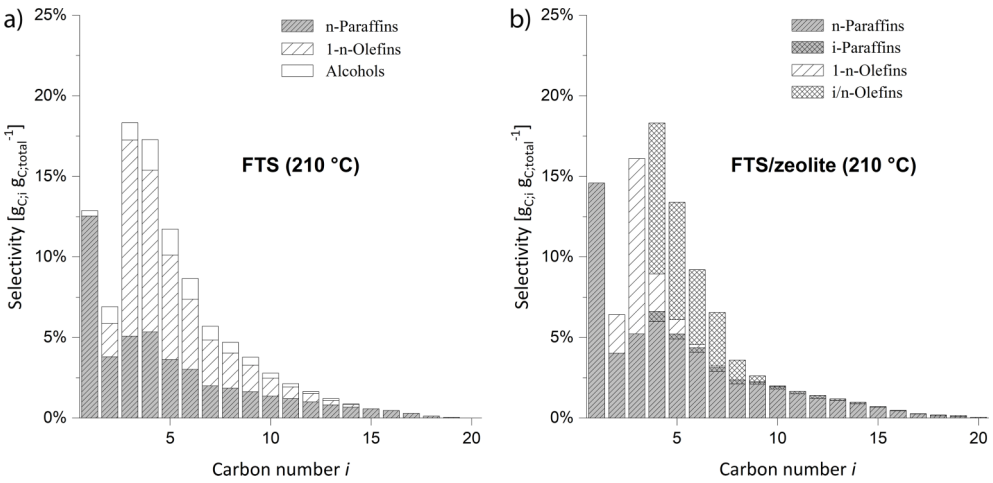


**Figure 4.** Comparison of HC distribution for (a) FTS at 210 °C and (b) FTS/zeolite in a dual-bed reactor at the same temperature. The denotation *i*-/*n*-olefins includes all branched and linear olefins except of the linear 1-olefins ($p_{total}$ = 20 bar, $p_{H2}/p_{CO}$ = 2, $m_{catalyst}$ = 2.5 g, $m_{zeolite}$ = 0.97 g, $X_{CO}$ = 12 %, $\tau^*_{zeolite}$ = 2.2 $kg_{zeolite}$ h $m^{-3}$).

  

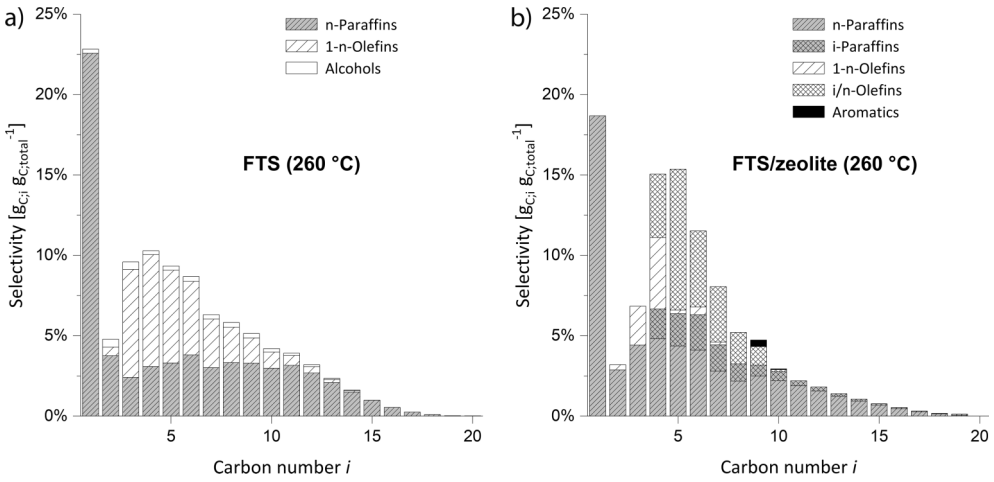


**Figure 5.** Comparison of HC distribution for (a) FTS at 260 °C and (b) FTS/zeolite in a dual-bed reactor at the same temperature ($p_{total} = 20$ bar, $p_{H2}/p_{CO} = 2$, $m_{catalyst} = 0.19$ g, $m_{zeolite} = 0.97$ g, $X_{CO} = 15$ %, $\tau^*_{zeolite} = 1.3\ kg_{zeolite} h\ m^{-3}$).

proportion of alkenes is present in the product spectrum than according to the thermodynamic equilibrium.

Duyckaerts et al. observed that at syngas conditions in FTS/zeolite reactions, the CO inhibits the (de)hydrogenation functionality by CO poisoning of metal sites, leading to divergences in the reaction pathways compared to conditions with $H_2$ only [31]. Furthermore, if the (de)hydrogenation activity is sufficiently high, long-chain products should no longer be present after passing the zeolite, since, from a thermodynamic point of view, the adsorption and conversion of olefins is more favorable with increasing chain length [39]. However, the selectivity of these long-chain hydrocarbons is almost unchanged compared to the FTS selectivity. From this it can be concluded that a weakening of the (de)hydrogenation component takes place.

Tab. 2 presents the HC selectivities for the temperature variation in the range from 210 °C to 270 °C of FTS and FTS/zeolite in the dual-bed setup. Within the experimental scatter of data, the selectivities of the FTS reaction compared with the FTS/zeolite reaction remain unchanged. Since the reaction was performed in a dual-bed setup and both catalysts are in the same reactor, the temperature and residence time of the FT reaction and cracking could not be adjusted independently. To ensure a constant conversion of CO in the FTS, a high volume flow of CO is required due to an increased CO reaction rate at the high temperature of 270 °C. According to this, also the residence time of primary FT products in the zeolite bed is reduced, which results in a decreased cracking rate. Because of the relatively low $\alpha$ values of the FTS, most primary FT products are in the range of $C_1$–$C_{15}$. If it is also taken into account that the reaction rate during cracking is strongly dependent on the chain length and decreases sharply with decreasing length [39], it can be explained that the FT products are (almost) not cracked under the conditions in the dual-bed arrangement.

The acidity of the zeolite was proofed by $NH_3$-TPD measurements showing two distinct $NH_3$ desorption peaks indication acid centers at the catalyst surface (see Fig. S5). A general inactivity of the zeolite for cracking reactions can be excluded since the same catalyst shows cracking activity in the tandem reactor setup at elevated temperature (see Fig. 6).

**Table 2.** HC selectivities of FTS and FTS/zeolite in a dual-bed setup.

| Temp. [°C] | Selectivity [$wt_C$ %] | | | |
|---|---|---|---|---|
| | $CH_4$ | $C_2$ | $C_{3+4}$ | $C_{5+}$ |
| *FTS only* | | | | |
| 210 | 12.5 | 6.8 | 36.4 | 44.3 |
| 220 | 15.3 | 6.7 | 35.3 | 42.7 |
| 230 | 17.7 | 7.1 | 33.0 | 42.2 |
| 250 | 20.7 | 5.0 | 22.4 | 51.9 |
| 260 | 22.6 | 4.8 | 20.0 | 52.6 |
| 270 | 25.6 | 4.9 | 18.6 | 50.9 |
| *FTS/zeolite* | | | | |
| 210 | 14.6 | 6.4 | 34.4 | 44.6 |
| 220 | 15.9 | 6.6 | 34.3 | 43.2 |
| 230 | 18.0 | 6.2 | 31.0 | 44.8 |
| 250 | 16.6 | 3.2 | 22.1 | 58.1 |
| 260 | 18.7 | 3.2 | 21.9 | 56.2 |
| 270 | 22.5 | 4.0 | 22.9 | 50.6 |

The temperature in the dual-bed setup was limited to 270 °C to avoid a temperature runaway of the FT reaction and also excessive unwanted methane formation. Therefore, both reactions were separated in two different, independently heated reactors (tandem configuration, Fig. 2b). In this case, the reaction temperature of the zeolite bed could be increased further at constant lower FTS temperature.

  

### 3.3 Product Composition at Constant FTS Temperature and Varying Cracking Temperature for Tandem Reactor Setup

For the tandem reactor setup both reactions (FTS and cracking) were carried out in two different reactors (see Fig. 2b). The FT reaction temperature was kept constant at 260 °C because of the high selectivity to long-chain HCs which can then be further cracked to achieve a higher overall LPG selectivity.

Fig. 6 depicts the selectivities for a varying cracking temperature in a range of 260 °C to 450 °C. Up to a temperature of 360 °C, the (overall) selectivity of LPG increased from initially 26 $wt_C$ %, reflecting the value achieved by FTS only, to 42 $wt_C$ %. A further temperature rise did not significantly increase the LPG yield, but results in a strong increase in methane selectivity. Also the selectivity for $C_2$-HCs almost linearly increased with rising temperature. The additional formation of methane and $C_2$ can be assigned to some superimposed Haag-Dessau [40] or thermal cracking at these high reaction temperatures (> 360 °C). Methanation of the syngas can also be a reason for the additional methane formed. The preferable cracking temperature for this reaction setup regarding a high (overall) LPG yield is therefore 360 °C. Even though a higher temperature decreases the $C_{5+}$ selectivity, it also leads to an unwanted increase in $C_1$ and $C_2$ compounds due to thermal cracking, Haag-Dessau cracking or methanation.

Fig. 7 shows the distribution of HCs for the FTS base run at 260 °C (Fig. 7a) and the tandem reactor setup at a cracking temperature of 360 °C (Fig. 7b). Intensive cracking of the long-chain products of primary FTS can be observed because almost no HCs with a carbon number *i* higher than 10 were detected. Compared to the FTS experiment only, the selectivity towards olefins drastically drops after passing the zeolite. This indicates an increased hydrogenation reactivity of the Pt at 360 °C compared to 260 °C (see Fig. 5). In addition, since almost all $C_{10+}$-HCs have now been cracked and paraffins must be activated before they can react, this supports the assumption that the (de)hydrogenation activity strongly increases. The still large presence of $C_5$ and $C_6$ olefins and paraffins in the product spectrum is attributed to bifunctional hydrocracking, in which HC with a chain length ≤ $C_6$ are cracked very slowly. Also, a not negligible amount of aromatics were present in the product spectrum, originating from dehydrocyclization reactions.

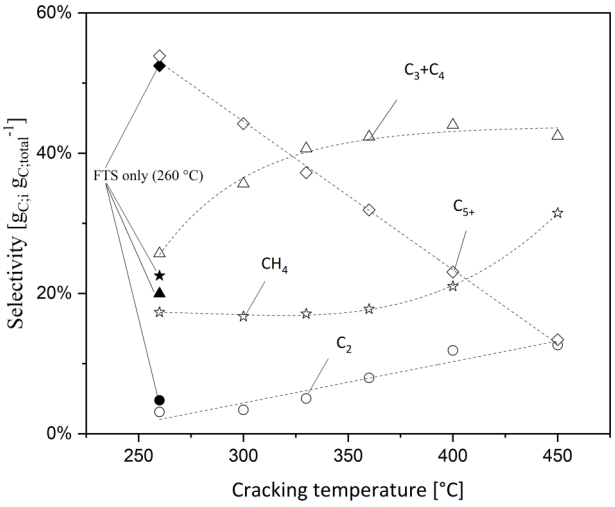


**Figure 6.** Selectivities for varying cracking temperatures at a constant FTS temperature (260 °C) for the tandem reactor setup. Filled data points show selectivities for only FTS reaction at 260 °C ($p_{total}$ = 20 bar, $p_{H2}/p_{CO}$ = 2, $m_{catalyst}$ = 0.19 g, $m_{zeolite}$ = 0.97 g, $X_{CO}$ = 15 %, $\tau^*_{zeolite}$ ($T$) = 0.92 $kg_{zeolite}$h $m^{-3}$ (450 °C) – 1.3 $kg_{zeolite}$h $m^{-3}$ (260 °C)).

### 3.4 Effect of Temperature on the Cracking of *n*-Hexadecane as Model Substance

To investigate the cracking reactions (only) in more detail and to find out the best conditions for a high cracking selectivity to LPG, *n*-hexadecane (*n*-$C_{16}$) was used as model substance for long-chain FT products. Furthermore, the mechanisms of hydrocracking on the bifunctional Pt/H-ZSM-5 zeolite should

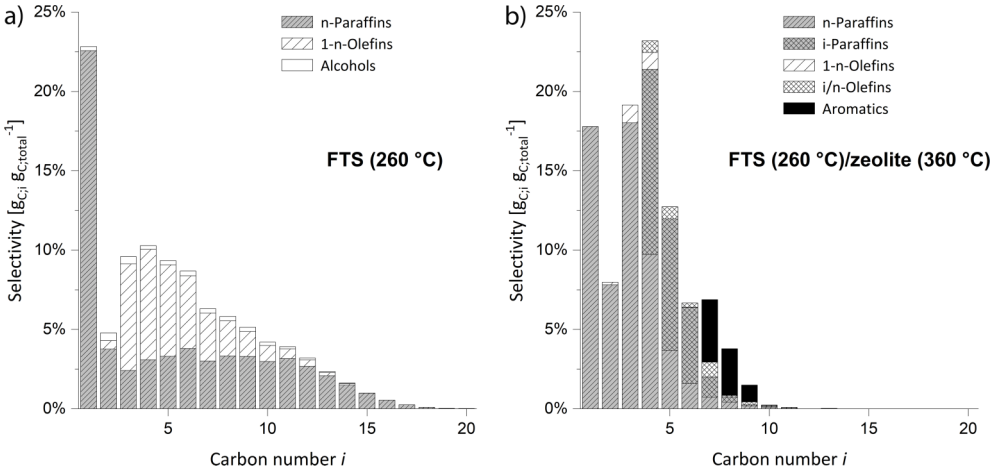


**Figure 7.** HC distribution of (a) FTS only at 260 °C and (b) tandem reactor setup with cracking at 360 °C ($p_{total}$ = 20 bar, $p_{H2}/p_{CO}$ = 2, $m_{catalyst}$ = 0.19 g, $m_{zeolite}$ = 0.97 g, $X_{CO}$ = 15 %, $\tau^*_{zeolite}$ = 1.3 $kg_{zeolite}$h $m^{-3}$).

  

be investigated to confirm the already obtained results of a decrease in the (de)hydrogenation activity.

Fig. 8 shows the HC distribution for the cracking at different temperatures. Even at the lowest temperature of 260 °C (conversion $X$ = 51 %) the product pattern of cracking was asymmetric with a majority of the products in the $C_3$–$C_5$ region, indicating that secondary cracking already occurs. For ideal hydrocracking (pure primary cracking) a bell-shaped molar distribution curve would be characteristic [13]. These curves are obtained for catalysts with a strong (de)hydrogenation activity and large enough pores to ensure a rapid desorption of the primary cracked products.

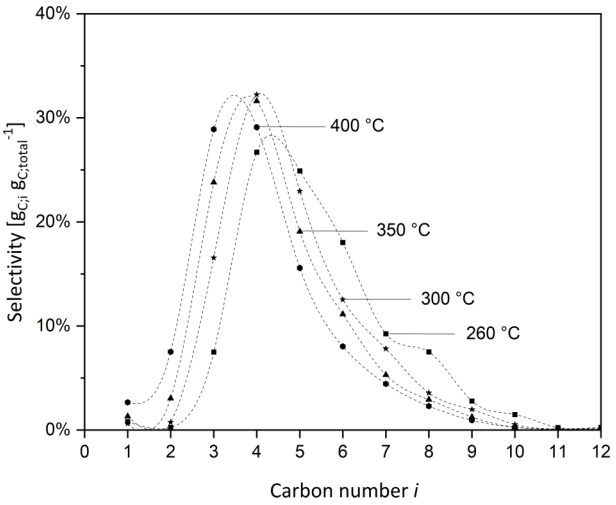


**Figure 8.** Distribution of HCs for different cracking temperatures of *n*-hexadecane ($p_{total}$ = 20 bar, $p_{H2}/p_{CO}$ = 2, $p_{n\text{–}hexadecane}$ = 0.14 bar, $m_{zeolite}$ = 0.97 g, $X_{n\text{-}hexadecane}$ ≈ const. = 51–65 %, $\tau^*_{zeolite}$ = 0.26 $kg_{zeolite}$h $m^{-3}$ (400 °C) – 2.84 $kg_{zeolite}$h $m^{-3}$ (260 °C)).

The deviation in shape of the product curve indicates a decrease of the (de)hydrogenation activity which could be already observed in FTS/zeolite experiments. This prolongs the residence time of carbocation intermediates on the acid sites of the catalyst, because of the lower number of olefins competing for active sites and secondary cracking reactions can then occur. Increasing the temperature at a constant *n*-$C_{16}$ conversion level shifted the maximum of the distribution curve to the left and also $C_1$- and $C_2$-HCs appear in significant amounts, indicating superimposed thermal or Haag-Dessau cracking at elevated temperatures. At increased temperatures also the slow type C $\beta$-scissions seems to take place and therefore decreases the $C_6$ selectivity in favor of an increasing $C_3$ selectivity.

Fig. 9 presents the selectivities for HCs at different cracking temperatures for the cracking of *n*-hexadecane at a constant conversion level. Up to a temperature of 350 °C, the selectivity for LPG increases and then remains fairly constant with further temperature increase. In the same way, the selectivity to the $C_{5+}$ products decreases with rising temperature, indicating an increased secondary cracking of the HCs on the zeolite. However, since thermal or Haag-Dessau cracking is also favored with higher temperature and more $C_1$ and $C_2$ products are formed, a temperature of 350 °C is considered to be the optimum temperature for maximizing the LPG yield. These results are in good agreement with FTS/zeolite experiments presented in Fig. 6.

## 4 Conclusions

It was found that a raise in temperature resulted in an increase of the chain growth probability $\alpha$ for FTS reaction on a Co/Mn catalyst. This also lowered the selectivity for the desired LPG. Since the maximal theoretical yield of LPG for FTS is limited due to the ASF distribution, a H-ZSM-5 zeolite was introduced for cracking longer HCs and by that, improving the overall LPG selectivity. In the dual-bed setup, i.e., at constant temperatures of FTS and cracking, the cracking reactions played only a minor role and did not further increase the LPG selectivity in a range of 210 °C to 260 °C. However, a certain conversion of FTS products, alcohol dehydration and isomerization of olefins, took place.

Integrating FTS and hydrocracking in a single reactor has the drawback that both catalysts must operate at the same temperature, i.e., at least in one case not at optimal reaction conditions. This problem can be circumvented by separating the combined reaction system in two separate reactors. A zeolite temperature of 360 °C was found to be optimal for achieving the highest overall selectivity for LPG of 42 $wt_C$ % with 260 °C for the upstream FTS. Besides bifunctional hydrocracking, also thermal and/or Haag-Dessau cracking contributed to cracking and $C_1$ and $C_2$-HCs were also produced to a small extent. In

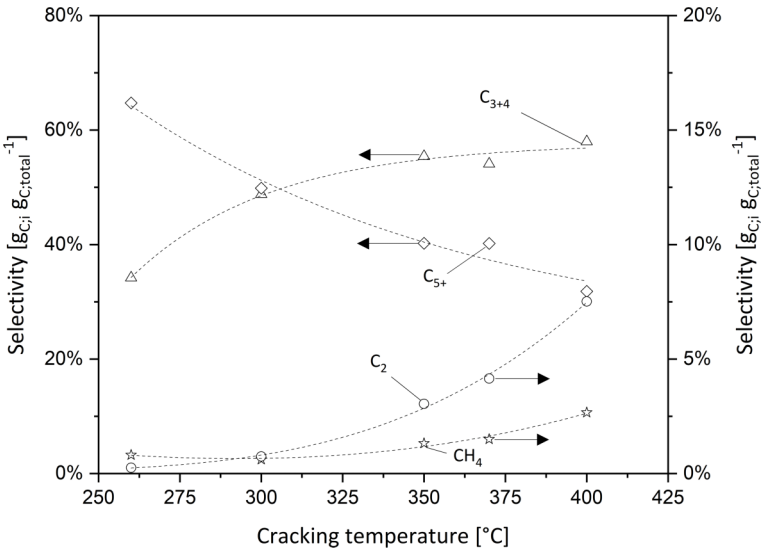


**Figure 9.** Selectivities of HCs for different cracking temperatures of *n*-hexadecane ($p_{total}$ = 20 bar, $p_{H2}/p_{CO}$ = 2, $p_{n\text{-}hexadecane}$ = 0.14 bar, $m_{zeolite}$ = 0.97 g, $X_{n\text{-}hexadecane}$ ≈ const. = 51–65 %, $\tau^*_{zeolite}$ = 0.26 $kg_{zeolite}$h $m^{-3}$ (400 °C) – 2.84 $kg_{zeolite}$h $m^{-3}$ (260 °C)).

  

addition, especially at higher temperatures, a not negligible amount of aromatics were formed.

To be able to investigate the cracking reactions independently of the FTS product spectrum, experiments were carried out using *n*-hexadecane as a model cracking substance. This confirmed the results already obtained. Also a temperature of around 350 °C was found as optimum cracking temperature, because a further increase in temperature lowered the selectivity of LPG due to the increased appearance of $C_1$- and $C_2$-HCs. Further studies are now conducted to evaluate the influence of CO and the gas compositions in general on the cracking reactions.

## Supporting Information

Supporting Information for this article can be found under DOI: https://doi.org/10.1002/ceat.202200445. This section includes additional references to primary literature relevant for this research [41–44].

## Acknowledgment

The authors thank the Oberfrankenstiftung for financial support. Open access funding enabled and organized by Projekt DEAL.

*The authors have declared no conflict of interest.*

## Symbols used

| | | |
|---|---|---|
| $d$ | [m] | diameter |
| $d_P$ | [m] | particle diameter |
| $F$ | [–] | pore filling degree |
| $L$ | [m] | length |
| $\dot{m}$ | [kg s$^{-1}$] | mass flow |
| $m$ | [kg] | mass |
| $\dot{n}$ | [mol s$^{-1}$] | molar flow |
| $p$ | [bar] | pressure |
| $S$ | [–] | selectivity |
| $T$ | [°C] | temperature |
| $\dot{V}$ | [m$^3$s$^{-1}$] | volume flow |
| $V$ | [m$^3$] | volume |
| $X$ | [–] | conversion |

*Greek letters*

| | | |
|---|---|---|
| $\alpha$ | [–] | chain growth probability factor |
| $\beta$ | [–] | beta position |
| $\rho$ | [kg m$^{-3}$] | density |
| $\tau^*$ | [kg$_{zeolite}$h m$^{-3}$] | modified residence time |
| $\omega$ | [–] | mass fraction |

*Sub- and superscripts*

| | |
|---|---|
| $C$ | carbon |
| $i$ | compound *i* |

*Abbreviations*

| | |
|---|---|
| ASF | Anderson-Schulz-Flory |
| FTS | Fischer-Tropsch synthesis |
| GC | gas chromatography |
| HCs | hydrocarbons |
| HPLC | high-performance liquid chromatography |
| H-ZSM-5 | zeolite socony mobil-5 (hydrogen form) |
| LPG | liquefied petroleum gas |
| PEM | proton exchange membrane |

## References

[1] *Renewable Energy Sources and Climate Change Mitigation*, Intergovernmental Panel on Climate Change, New York **2012**.
[2] M. E. Dry, *Catal. Today* **2002**, *71 (3–4)*, 227–241. DOI: https://doi.org/10.1016/S0920-5861(01)00453-9
[3] P. Kaiser, R. B. Unde, C. Kern, A. Jess, *Chem. Ing. Tech.* **2013**, *85 (4)*, 489–499. DOI: https://doi.org/10.1002/cite.201200179
[4] Z. Gholami, Z. Tišler, V. Rubáš, *Catal. Rev.* **2021**, *63 (3)*, 512–595. DOI: https://doi.org/10.1080/01614940.2020.1762367
[5] F. Fischer, H. Tropsch, *Ber. Dtsch. Chem. Ges.* **1926**, *59 (4)*, 830–831. DOI: https://doi.org/10.1002/cber.19260590442
[6] A. Y. Krylova, *Solid Fuel Chem.* **2014**, *48 (1)*, 22–35. DOI: https://doi.org/10.3103/S0361521914010030
[7] S. S. Ail, S. Dasappa, *Renewable Sustainable Energy Rev.* **2016**, *58*, 267–286. DOI: https://doi.org/10.1016/j.rser.2015.12.143
[8] D. Spohn, *Energy & Management Powernews* **2021**, July 12.
[9] G. Henrici-Olivé, S. Olivé, *Angew. Chem., Int. Ed.* **1976**, *15 (3)*, 136–141. DOI: https://doi.org/10.1002/anie.197601361
[10] N. O. Elbashir, C. B. Roberts, *Ind. Eng. Chem. Res.* **2005**, *44 (3)*, 505–521. DOI: https://doi.org/10.1021/ie0497285
[11] P. Lu, J. Sun, D. Shen, R. Yang, C. Xing, C. Lu, N. Tsubaki, S. Shan, *Appl. Energy* **2018**, *209*, 1–7. DOI: https://doi.org/10.1016/j.apenergy.2017.10.068
[12] H. Kirsch, L. Brübach, M. Loewert, M. Riedinger, A. Gräfenhahn, T. Böltken, M. Klumpp, P. Pfeifer, R. Dittmeyer, *Chem. Ing. Tech.* **2020**, *92 (1–2)*, 91–99. DOI: https://doi.org/10.1002/cite.201900120
[13] A. V. Karre, A. Kababji, E. L. Kugler, D. B. Dadyburjor, *Catal. Today* **2012**, *198 (1)*, 280–288. DOI: https://doi.org/10.1016/j.cattod.2012.04.068
[14] Q. Zhang, K. Cheng, J. Kang, W. Deng, Y. Wang, *ChemSusChem* **2014**, *7 (5)*, 1251–1264. DOI: https://doi.org/10.1002/cssc.201300797
[15] S. Sartipi, M. Makkee, F. Kapteijn, J. Gascon, *Catal. Sci. Technol.* **2014**, *4 (4)*, 893–907. DOI: https://doi.org/10.1039/C3CY01021J
[16] A. A. Adeleke, X. Liu, X. Lu, M. Moyo, D. Hildebrandt, *Rev. Chem. Eng.* **2020**, *36 (4)*, 437–457. DOI: https://doi.org/10.1515/revce-2018-0012
[17] R. L. Varma, N. N. Bakhshi, J. F. Mathews, S. H. Ng, *Ind. Eng. Chem. Res.* **1987**, *26 (2)*, 183–188. DOI: https://doi.org/10.1021/ie00062a001

  

[18] A. Freitez, K. Pabst, B. Kraushaar-Czarnetzki, G. Schaub, *Ind. Eng. Chem. Res.* **2011**, *50 (24)*, 13732–13741. DOI: https://doi.org/10.1021/ie201913s
[19] K. Pabst, B. Kraushaar-Czarnetzki, G. Schaub, *Ind. Eng. Chem. Res.* **2013**, *52 (26)*, 8988–8995. DOI: https://doi.org/10.1021/ie3030483
[20] S. T. Sie, M. Senden, H. van Wechem, *Catal. Today* **1991**, *8 (3)*, 371–394. DOI: https://doi.org/10.1016/0920-5861(91)80058-H
[21] S. Wang, Q. Yin, J. Guo, B. Ru, L. Zhu, *Fuel* **2013**, *108*, 597–603. DOI: https://doi.org/10.1016/j.fuel.2013.02.021
[22] Y.-P. Li, T.-J. Wang, C.-Z. Wu, X.-X. Qin, N. Tsubaki, *Catal. Commun.* **2009**, *10 (14)*, 1868–1874. DOI: https://doi.org/10.1016/j.catcom.2009.06.021
[23] F. Botes, W. Böhringer, *Appl. Catal., A* **2004**, *267 (1–2)*, 217–225. DOI: https://doi.org/10.1016/j.apcata.2004.03.006
[24] S.-H. Kang, J.-H. Ryu, J.-H. Kim, I. H. Jang, A. R. Kim, G. Y. Han, J. W. Bae, K.-S. Ha, *Energy Fuels* **2012**, *26 (10)*, 6061–6069. DOI: https://doi.org/10.1021/ef301251d
[25] K. M. Cho, S. Park, J. G. Seo, M. H. Youn, S.-H. Baeck, K.-W. Jun, J. S. Chung, I. K. Song, *Appl. Catal., B* **2008**, *83 (3–4)*, 195–201. DOI: https://doi.org/10.1016/j.apcatb.2008.02.022
[26] A. Corsaro, T. Wiltowski, D. Juchelkova, S. Honus, *Pet. Sci. Technol.* **2014**, *32 (20)*, 2497–2505. DOI: https://doi.org/10.1080/10916466.2013.845574
[27] E. Blomsma, J. A. Martens, P. A. Jacobs, *J. Catal.* **1997**, *165 (2)*, 241–248. DOI: https://doi.org/10.1006/jcat.1997.1473
[28] J. Weitkamp, *ChemCatChem* **2012**, *4 (3)*, 292–306. DOI: https://doi.org/10.1002/cctc.201100315
[29] A. Martinez, J. Rollan, M. Arribas, H. Cerqueira, A. Costa, E. Saguiar, *J. Catal.* **2007**, *249 (2)*, 162–173. DOI: https://doi.org/10.1016/j.jcat.2007.04.012
[30] D. Schröder, J. Thiessen, A. Jess, J. Scholz, *Catal. Sci. Technol.* **2020**, *10 (2)*, 475–483. DOI: https://doi.org/10.1039/C9CY02022E
[31] N. Duyckaerts, I.-T. Trotuş, A.-C. Swertz, F. Schüth, G. Prieto, *ACS Catal.* **2016**, *6 (7)*, 4229–4238. DOI: https://doi.org/10.1021/acscatal.6b00904
[32] G. P. van der Laan, A. A. C. M. Beenackers, *Catal. Rev.* **1999**, *41 (3–4)*, 255–318. DOI: https://doi.org/10.1081/CR-100101170
[33] D. Vervloet, F. Kapteijn, J. Nijenhuis, J. R. van Ommen, *Catal. Sci. Technol.* **2012**, *2 (6)*, 1221. DOI: https://doi.org/10.1039/C2CY20060K
[34] E. Iglesia, S. L. Soled, R. A. Fiato, G. H. Via, *J. Catal.* **1993**, *143 (2)*, 345–368. DOI: https://doi.org/10.1006/jcat.1993.1281
[35] E. Iglesia, *J. Catal.* **1991**, *129 (1)*, 238–256. DOI: https://doi.org/10.1016/0021-9517(91)90027-2
[36] B. W. Wojciechowski, *Catal. Rev.* **1988**, *30 (4)*, 629–702. DOI: https://doi.org/10.1080/01614948808071755
[37] H. Schulz, K. Beck, E. Erich, in *Studies in Surface Science and Catalysis* (Eds: D. M. Bibby, C. D. Chang, R. F. Howe, S. Yurchak), Vol. 36, Elsevier, Oxford **1988**.
[38] P. Rausch, Hydrocracken von Fischer-Tropsch-Wachsen mit Polyoxometallaten als Katalysator, *Ph.D. Thesis*, Universität Bayreuth **2021**.
[39] K. Hedden, J. Weitkamp, *Chem. Ing. Tech.* **1975**, *47 (12)*, 505–513. DOI: https://doi.org/10.1002/cite.330471202
[40] S. Kotrel, H. Knözinger, B. C. Gates, *Microporous Mesoporous Mater.* **2000**, *35–36*, 11–20. DOI: https://doi.org/10.1016/S1387-1811(99)00204-8
[41] J. G. Post, J. van Hooff, *Zeolites* **1984**, *4 (1)*, 9–14. DOI: https://doi.org/10.1016/0144-2449(84)90065-4
[42] A. S. Al-Dughaither, H. de Lasa, *Ind. Eng. Chem. Res.* **2014**, *53 (40)*, 15303–15316. DOI: https://doi.org/10.1021/ie4039532
[43] S. Rößler, C. Kern, A. Jess, *Chem. Ing. Tech.* **2018**, *90 (5)*, 634–642. DOI: https://doi.org/10.1002/cite.201700142
[44] F. Pöhlmann, C. Kern, S. Rößler, A. Jess, *Catal. Sci. Technol.* **2016**, *6 (17)*, 6593–6604. DOI: https://doi.org/10.1039/C6CY00941G

  